NUMERICAL STUDY OF MAGNETOHYDRODYNAMIC MIXED CONVECTIVE FLOW IN A LID-DRIVEN ENCLOSURE FILLED WITH NANOFLUID SATURATED POROUS MEDIUM WITH CENTER HEATER

by

Thangavelu MAHALAKSHMI [a*], ***Nagarajan NITHYADEVI*** [a], ***and Hakan F. OZTOP*** [b]

[a] Department of Mathematics, Bharathiar University, Coimbatore, Tamil Nadu, India
[b] Department of Mechanical Engineering, Firat University, Elazig, Turkey

Original scientific paper
https://doi.org/10.2298/TSCI171105313N

This present numerical study explores the MHD mixed convective flow and heat transfer analysis in a square porous enclosure filled with nanofluid having center thin heater. The left and right walls of the enclosure are maintained at temperature T_c. The bottom wall is considered with a constant heat source whereas the remaining part of bottom wall and top wall are kept adiabatic. The finite volume method based on SIMPLE algorithm is used to solve the governing equations in order to investigate the effect of heater length, Hartmann, Richardson, and Darcy numbers on the fluid-flow and heat transfer characteristics inside the enclosure. A set of graphical results are presented in terms of streamlines, isotherms, mid height velocity profiles and average Nusselt numbers. The results reveal that heat transfer rate increases as heater length increases for increasing Darcy and Richardson numbers. Among the two positions of heaters, larger enhancement of heat transfer is obtained for horizontal heater of maximum length. It is observed that, Hartmann number is a good control parameter for heat transfer in fluid-flow through porous medium in enclosure. Moreover, Ag-water nanofluid has greater merit to be used for heat transfer enhancement. This problem may be occurred in designing cooling system for electronic equipment to maximize the efficiency with active and secured operational conditions.

Key words: *mixed convection, magnetic field, square enclosure, porous medium, nanofluid-flow, center heater.*

Introduction

In recent years, mixed convective heat transfer in porous media has received more attention due to its importance in many engineering applications. These applications include porous insulation, packed bed reactors, electronic device cooling, coating, nuclear waste disposal, food processing, grain storage, and geophysics. The fundamental study concerning convective flow in porous media and their application areas in the real life are clearly found in the books by [1-4]. Various studies on mixed convection were carried out in a lid-driven enclosure filled with porous medium for its applications [5-7]. Basak *et al*. [8] investigated mixed convective flow in a lid-driven porous enclosure with two different types of heating on bottom wall and their results showed that enhanced heat transfer rate is obtained for higher values of pertinent parameters concerned. Rahman *et al*. [9] performed a numerical study on mixed convection flow in a porous enclosure with two isothermal curvilinear heaters on bottom wall.

Corresponding author, e-mail: saimaha13@gmail.com

They obtained the results that heat transfer decreases with decreasing Darcy effect and curvilinear heaters having small diameter produces small significant effect on mixed convection. In the literature review, researchers analyzed mixed convection in an enclosure with porous medium on different lid-driven boundary conditions.

As working fluids having low thermal properties are a main limitation, adding small nanoparticles into the base fluid is an innovative way to improve the heat transfer. Mittal *et al*. [10] conducted numerical simulation on mixed convection in an enclosure with porous medium filled with Al_2O_3-water nanofluid and they observed from their results that heat transfer increases with increasing Darcy effect and by adding Al_2O_3 nanoparticles to the base fluid in porous medium. Heydari *et al*. [11] studied mixed convection of Cu-water nanofluid in a double lid-driven inclined enclosure. They showed that increasing volume fraction of nanoparticles, ϕ, for a constant Richardson number enhances rate of heat transfer whereas decreasing Richardson number for a particular, φ, enhances heat transfer. Similar way, mixed convective nanofluid flow in a two sided lid-driven square enclosure in the presence of magnetic field was explored by Kefayati [12]. He observed the influence of nanoparticle on heat transfer and obtained that increasing magnetic field effect decreases the heat transfer in the enclosure. Mixed convection and entropy generation of Cu-water nanofluid was studied by Nayak *et al*. [13]. They found that higher rate of heat transfer enhancement compared with the augmentation rate in entropy generation obtained for wide range of Reynolds and Grashof numbers.

Heat transfer inside a porous complex shaped enclosure filled with Fe_3O_4-water was investigated by Sheikholeslami [14]. It was observed from their results that effect of Hartmann number on heat transfer rate is more observable in medium with higher permeability. Sheikholeslami and Rokni [15] analyzed the behaviour of nanofluid for the enhancement of heat transfer inside the enclosure in the presence of magnetic field. They found that both single and two phase ways are essential. But as far as interaction between base fluid and nanoparticle concerned two phase model is better. Sheikholeslami and Bhatti [16] examined the MHD forced convective heat transfer inside a porous semi-annulus. They obtained heat transfer enhances with increasing volume fraction of nanofluid, Reynolds and Darcy numbers whereas it reduces with increasing effect of magnetic field.

In order to enhance the heat transfer, the most important method is to consider the heat source inside the enclosure. Oztop *et al*. [17] investigated the effect of both positions and aspect ratio of heated plate inside enclosure. They found that high heat transfer enhancement was obtained by locating heated plate at vertical position than the horizontal one. In the following, authors considered the enclosure with different types of heat source to investigate mixed convection in enclosure to achieve high heat transfer for their applications in equipment cooling, food preservation and processing, *etc*., Dogan and Sivrioglu [18] studied the mixed convection from a longitudinal fin in a horizontal rectangular enclosure. They showed the result that optimum fin spacing yields the maximum heat transfer depend on its height. Islam *et al*. [19] examined mixed convection flow in a lid-driven enclosure with square block and circular cylinder in their investigations.

After that, enclosure containing nanofluid with detached obstacle of different shapes had been investigated for mixed convective heat transfer by Kalteh *et al*. [20]. Even though, more literature revealing characteristics of mixed convection in an enclosure with obstacle of various shapes is available, only little is identified regarding the MHD mixed convection in lid-driven enclosure with different heat sources. Rahman *et al.* [21] studied MHD mixed convection flow in a lid-driven enclosure with a heated semicircular object on right wall and they observed that heat transfer decreased with increasing magnetic field effect and decreasing Joule heating parameter.

In a similar way, MHD mixed convection in an enclosure with a hot circular solid object and rotating cylinder was investigated by Selimefendigil and Oztop [22]. Recently, Abu Nada [23] conducted dissipative particle dynamics simulation to investigate mixed convective flow and heat transfer in a vertical lid-driven enclosure with a corner heater.

Rahman *et al*., [24] analyzed the mixed convection in porous enclosure with semicircular heater and found that heat transfer decreases with decrease of Darcy and Richardson numbers whereas the strength of flow increases with increase of tine increment. Currently, mixed convection in a top lid-driven enclosure having triangular block with constant heat flux condition is delineated by Gangawane [25]. It is observed from his analyses that insertion of triangular block is appropriate to control the convective fluid flow and heat transfer inside the lid-driven enclosure. Nanofluid heat transfer enhancement in the presence of magnetic field concern with impact of melting heat transfer has been numerically investigated by Sheikholeslami and Sadonghi [26]. Their results showed that heat transfer augments with increasing melting parameter, Rayleigh number and CuO-water volume fraction. But heat transfer detracts with increasing magnetic field effect.

To the best of authors understanding, little attention is given to the problem of MHD mixed convective heat transfer in a lid-driven enclosure with detached heat sources. There is no study on MHD mixed convective nanofluid flow in porous enclosure with center heater. Therefore, this problem could be occurred in many engineering applications such as evaporative cooling and solidification, enhanced oil recovery, cooling of electronic device and nuclear reactors. The objective of the present study is to investigate numerically MHD mixed convection of nanofluid flow in a vertically lid-driven porous enclosure with center heater. Numerical results are presented via streamlines, isotherms, velocity profiles and average Nusselt numbers to analyze the effects of heater length, Richardson, Darcy, and Hartmann numbers on the fluid-flow and heat transfer.

Problem statement

A schematic description of the lid driven porous enclosure with center heater is shown in fig. 1. The height and width of the square enclosure are denoted by L. Both left and right vertical walls are moving in the opposite direction with same velocity. The gravity acts in the negative y-direction. The uniform external magnetic field of constant strength, B_0, is applied in the x-direction. The vertical walls are maintained at low temperature, T_c , whereas a constant heat source is considered at the bottom wall and the remaining parts of bottom wall and the top wall are kept adiabatic. A thin center heater with temperature, T_h, is located inside the enclosure at vertical and horizontal positions. In this figure γ represents the length of center heater, γ_1 represents the distance of heater to the parallel upper wall for first situation and the parallel left wall for the second situation, γ_2 is the distance of center of heater to the perpendicular left wall for the first situation and to perpendicular upper wall for second situation. These parameters are defined:

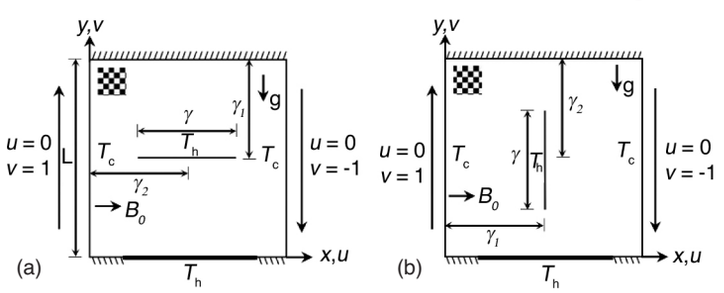

Figure 1. Physical configuration (a) horizontal ceneter heater, (b) vertical center heater

$$\Gamma = \frac{\gamma}{L},\ \Gamma_1 = \frac{\gamma_1}{L} \text{ and } \Gamma_2 = \frac{\gamma_2}{L}$$

Also, in this entire study both horizontal and vertical heater are considered at center position (*i. e.*, $\Gamma_1 = \Gamma_2 = 0.5$)

The enclosure is filled with Ag-water nanofluid under the influence of magnetic field. The nanofluid is assumed to be Newtonian, incompressible and the nanofluid flow is conceived as laminar and 2-D. Also it is assumed that both base fluid (water) and nanoparticles are in thermal equilibrium and there is no slip between them. The thermophysical properties of nanoparticles and water are presented in tab. 1. It is further assumed that the thermophysical properties of the nanofluid are constant with the exception of density which varies according to the Boussinesq approximation.

Table 1. Thermophysical properties of base fluid and solid nanoparticles. Mahmoodi [27]

Physical properties	Fluid phase (water)	Solid
c_p [J/kg/K]	4179	235
ρ [kg/m^3]	997.1	10500
k [W/mk]	0.613	429
$\beta \cdot 10^5$[k^{-1}]	21	1.89
$\sigma \cdot 10^7$[S/m]	0.05	6.30

Darcy model is invoked to represent the mixed convection within the porous medium. However, we have neglected Forchheimer inertia term in this present study as we deal with the mixed convection nanofluid flow in an enclosure filled with a porous medium under the effect of magnetic field.

Mathematical formulation

The governing equations (continuity, momentum, and energy equations) for a steady 2-D MHD mixed convective flow in a vertical lid-driven porous square enclosure are expressed:

$$\frac{\partial u}{\partial x} + \frac{\partial v}{\partial y} = 0 \tag{1}$$

$$u\frac{\partial u}{\partial x} + \frac{\partial v}{\partial y} = -\frac{1}{\rho_{nf}}\frac{\partial \rho}{\partial x} + \frac{\mu_{nf}}{\rho_{nf}}\nabla^2 u - \frac{\mu_{nf}}{\rho_{nf}}\frac{u}{k} \tag{2}$$

$$u\frac{\partial v}{\partial x} + \frac{\partial v}{\partial y} = -\frac{1}{\rho_{nf}}\frac{\partial \rho}{\partial y} + \frac{\mu_{nf}}{\rho_{nf}}\nabla^2 v - \frac{\mu_{nf}}{\rho_{nf}}\frac{v}{k} + \beta_{nf}\, g\, (T - T_c) - \frac{\sigma_{nf}}{\rho_{nf}} B_0{}^2 v \tag{3}$$

$$u\frac{\partial T}{\partial x} + v\frac{\partial T}{\partial y} = \alpha_{nf}(\nabla^2 T) \tag{4}$$

The boundary conditions for eqs. (1)-(4) are:

$$u = 0,\ v = 1,\ T = T_c \text{ at } x = 0 \text{ and } 0 \le y \le L$$

$$u = 0,\ v = -1,\ T = T_c \text{ at } x = L \text{ and } 0 \le y \le L$$

$$u = v = 0,\ \frac{\partial T}{\partial y} = 0 \text{ at } y = 0,\ 0 \le x < \frac{L-l}{2}, \frac{L+l}{2} < x \le L$$

$$u = v = 0,\ T = T_h \text{ at } y = 0,\ \frac{L-l}{2} \le x \le \frac{L+l}{2}$$

$$u = v = 0,\ \frac{\partial T}{\partial y} = 0 \text{ at } y = L,\ 0 \le x \le L$$

and on the heater:

$$u = v = 0, T = T_h,\ \gamma = \Gamma L,\ \gamma_1 = \Gamma_1 L, \text{ and } \gamma_2 = \Gamma_2 L \tag{5}$$

where the effective density and heat capacity of the nanofluid are calculated from the following equations:

$$\rho_{nf} = (1 - \varphi)\,\rho_f + \varphi\rho_s \tag{6}$$

Under the thermal equilibrium conditions, the specific heat of nanofluid is given:

$$(\rho c_p)_{\mathrm{nf}} = (1-\varphi)\,(\rho c_p)_{\mathrm{f}} + \varphi(\rho c_p)_{\mathrm{s}} \tag{7}$$

The thermal expansion coefficient of the nanofluid can be obtained from:

$$(\rho\beta)_{\mathrm{nf}} = (1-\varphi)\,(\rho\beta)_{\mathrm{f}} + \varphi(\rho\beta)_{\mathrm{s}} \tag{8}$$

The thermal diffusivity of the nanofluid is:

$$\alpha_{\mathrm{nf}} = \frac{k_{\mathrm{nf}}}{(\rho c_p)_{\mathrm{nf}}} \tag{9}$$

In this study the Brinkman model is used for the viscosity of the nanofluid. So the effective dynamic viscosity of the nanofluid is obtained from the formula:

$$\mu_{\mathrm{nf}} = \mu_{\mathrm{f}}\,(1-\varphi)^{-2.5} \tag{10}$$

The effective thermal conductivity of the nanofluid is determined by using the Maxwell model. For the suspension of spherical nanoparticles in the base fluid, it is written:

$$\frac{k_{\mathrm{nf}}}{k_{\mathrm{f}}} = \frac{(k_{\mathrm{s}} + 2k_{\mathrm{f}}) - 2\varphi\,(k_{\mathrm{f}} - k_{\mathrm{s}})}{(k_{\mathrm{s}} + 2k_{\mathrm{f}}) + \varphi\,(k_{\mathrm{f}} - k_{\mathrm{s}})} \tag{11}$$

Also the electrical conductivity of the nanofluid is given:

$$\sigma_{\mathrm{nf}} = (1-\varphi)\,\sigma_{\mathrm{f}} + \varphi\sigma_{\mathrm{s}} \tag{12}$$

Using the following dimensionless parameters, the governing equations can be converted to dimensionless forms:

$$\begin{gathered} X = \frac{x}{L},\ Y = \frac{y}{L},\ U = \frac{u}{V_0},\ V = \frac{v}{V_0},\ P = \frac{p}{\rho_{\mathrm{nf}} V_0^2},\ \theta = \frac{T - T_{\mathrm{c}}}{T_{\mathrm{h}} - t_{\mathrm{c}}},\ \mathrm{Gr} = \frac{\mathrm{g}\beta_f \Delta T L^3}{\upsilon_{\mathrm{f}}^2} \\ \mathrm{Re} = \frac{V_0 L}{\upsilon_f},\ \mathrm{Ri} = \frac{\mathrm{Gr}}{\mathrm{Re}^2},\ \mathrm{Pr} = \frac{\upsilon_{\mathrm{f}}}{\alpha_{\mathrm{f}}},\ \mathrm{Ha} = B_0 L \sqrt{\sigma_{\mathrm{nf}}/\rho_{\mathrm{nf}}\upsilon_{\mathrm{f}}},\ \mathrm{Da} = \frac{K}{L^2} \end{gathered} \tag{13}$$

By using the dimensionless variables, the governing eqs. (1)-(4) in dimensionless forms are:

$$\frac{\partial U}{\partial X} + \frac{\partial V}{\partial Y} = 0 \tag{14}$$

$$U\frac{\partial U}{\partial X} + V\frac{\partial U}{\partial Y} = -\frac{\partial P}{\partial X} + \frac{\mu_{\mathrm{nf}}}{\rho_{\mathrm{nf}}\upsilon_{\mathrm{f}}}\frac{1}{\mathrm{Re}}\nabla^2 U - \frac{\mu_{\mathrm{nf}}}{\rho_{\mathrm{nf}}\upsilon_{\mathrm{f}}}\frac{U}{\mathrm{ReDa}} \tag{15}$$

$$U\frac{\partial V}{\partial X} + V = \frac{\partial V}{\partial Y} = -\frac{\partial P}{\partial Y} + \frac{\mu_{\mathrm{nf}}}{\rho_{\mathrm{nf}}\upsilon_{\mathrm{f}}}\frac{1}{\mathrm{Re}}\nabla^2 V - \frac{\mu_{\mathrm{nf}}}{\rho_{\mathrm{nf}}\upsilon_{\mathrm{f}}}\frac{V}{\mathrm{ReDa}} + \frac{\beta_{\mathrm{nf}}}{\beta_{\mathrm{f}}}\frac{\mathrm{Gr}}{\mathrm{Re}^2}\theta - \frac{\mathrm{Ha}^2}{\mathrm{Re}}V \tag{16}$$

$$U\frac{\partial \theta}{\partial X} + V = \frac{\partial \theta}{\partial Y} = \frac{\alpha_{\mathrm{nf}}}{\alpha_{\mathrm{f}}}\frac{1}{\mathrm{RePr}}\nabla^2\theta \tag{17}$$

The boundary conditions for eqs. (14)-(17) are:

$$\begin{gathered} U = 0,\ V = 1,\ \theta = 0 \text{ at } X = 0 \text{ and } 0 \le Y \le 1 \\ U = 0,\ V = -1,\ \theta = 0 \text{ at } X = 1 \text{ and } 0 \le Y \le 1 \\ U = V = 0,\ \frac{\partial\theta}{\partial Y} = 0 \text{ at } Y = 0,\ 0 \le Y < \frac{1-\varepsilon}{2}, \frac{1+\varepsilon}{2} < X \le 1 \\ U = V = 0,\ \theta = 1 \text{ at } Y = 0, \text{ and } \frac{1-\varepsilon}{2} \le X \le \frac{1+\varepsilon}{2} \\ U = V = 0,\ \frac{\partial\theta}{\partial Y} = 0 \text{ at } Y = 1, \text{ and } 0 \le X \le 1 \end{gathered}$$

and on the heater:

$$U = V = 0,\ \theta = 1,\ \Gamma = \frac{\gamma}{L},\ \Gamma_1 = \frac{\gamma_1}{L}, \text{ and } \Gamma_2 = \frac{\gamma_2}{L} \tag{18}$$

The local Nusselt number along the vertical walls of an enclosure can be written:

$$\mathrm{Nu}\ (\mathrm{Y}) = -\frac{k_{\mathrm{nf}}}{k_{\mathrm{f}}}\left(\frac{\partial\theta}{\partial X}\right)_{X=0,1}$$

The average Nusselt number is calculated by integrating the local Nusselt number along the vertical walls:

$$\overline{\mathrm{Nu}}\ (Y) = \frac{1}{2}\left[\left(\int_0^1 \mathrm{Nu}\ (Y)\ (\mathrm{d}Y)_{X=0}\right) + \left(\int_0^1 \mathrm{Nu}\ (Y)\ (\mathrm{d}Y)_{X=1}\right)\right]$$

$$\mathrm{Nu}\ (X) = -\frac{k_{\mathrm{nf}}}{k_{\mathrm{f}}}\left(\frac{\partial\theta}{\partial Y}\right)_{Y=0}$$

For the bottom wall

$$\overline{\mathrm{Nu}}\ (X) = \int_{\frac{1-\varepsilon}{2}}^{\frac{1+\varepsilon}{2}} \mathrm{Nu}\ (X)\ \mathrm{d}X$$

where ε is length of bottom heat source.

Numerical approach

The governing equations are discretized by using the finite volume method while the coupling between the velocity and pressure fields is done by using the SIMPLE algorithm of Patankar [28]. The diffusion terms in the equations are discretized by central different scheme, while a power law scheme [29-31] is applied to approximate the convection terms. The set of discretized algebraic equations are solved by tridiagonal matrix algorithm (TDMA) line by line method. The convergence criterion used for the field variables φ (= U, V, T) is:

$$\left|\frac{\varphi_{n+1}\ (i,j) - \varphi_n\ (i,j)}{\varphi_{n+1}\ (i,j)}\right| \le 10^{-5}$$

here the subscript n denotes the previous calculation and n+1 denoted the current calculation in iteration. The variables i, j denotes X- and Y-directional nodes in the computational domain.

Grid independence test and code validation

In order to conduct the grid independency study, the present developed FORTRAN code is tested for grid independency with seven different uniform grid size ranging from 21 × 21 to 141 × 141, tab. 2. for calculating the average Nusselt number on side walls. The significant changes occur in the average Nusselt number for grid size varies from 21 × 21 to 121 × 121 and for grid size 121 × 121 to 141 × 141 the average Nusselt number remains unchanged. Hence, it is found that a uniform grid size of 121 × 121 ensures the grid independence for all the subsequent numerical calculations, fig. 2. In order to validate the numerical code, three different test cases are employed using the present code and the results are compared with the existing results in the literature. The first test case is natural convection of pure water in a square enclosure with center heater. The obtained results by the present code are compared with results of Mahmoodi [27] shown in tab. 3.

Table 2. Grid independence test for vertical heater of length Γ = 0.5, Ra = 10^4, ε = 0.8, and φ = 0.06

Grid size	$\overline{\mathrm{Nu}}$	Error %
21 × 21	3.093351	13.16
41 × 41	3.562338	2.050
61 × 61	3.636895	0.668
81 × 81	3.661375	0.292
101 × 101	3.672102	0.124
121 × 121	3.676670	0.002
141 × 141	3.676780	

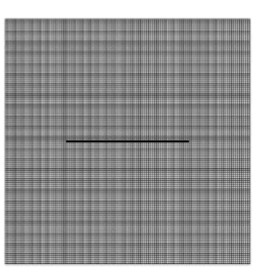

Figure 2. 121 × 121 grid

The second test case is natural convection of Al_2O_3-water nanofluid filled enclosure under the magnetic field effect at

Table 3. Comparison of average Nusselt numbers of cold side wall of square enclosure with an inside vertical heater with a length and location of 0.5 filled with pure waterat Ra = 10^6.

Grid size	21 × 21	41 × 41	61 × 61	81 × 81	101 × 101	121 × 121
[27]	4.1286	5.7732	6.9498	6.9545	6.9577	6.9591
Present study	4.128298	5.736319	6.926877	6.995508	6.970670	6.969583
Difference	0.000302	0.036881	0.022923	0.041008	0.012970	0.010483

Table 4. Comparison of $\overline{Nu}$ for different Rayleigh numbers and φ at Ha = 30 between present results and data of Ghasemi *et al.* [32]

Ra	φ	$\overline{Nu}$ [32]	Obtained results
10^3	0	1.002	1.045249
	0.02	1.060	1.049591
	0.04	1.121	1.108222
	0.06	1.184	1.154937
10^4	0	1.183	1.175236
	0.02	1.212	1.193954
	0.04	1.249	1.189233
	0.06	1.291	1.238562
10^5	0	3.150	3.096256
	0.02	3.138	3.087560
	0.04	3.124	3.080359
	0.06	3.108	3.089125
10^6	0	7.907	7.895364
	0.02	7.979	7.928563
	0.04	8.042	8.019586
	0.06	8.098	8.045284

Table 5. Comparison of Nu at the hot wall between the present results and data of Cheng and Liu [33]

Ri		$\overline{Nu}_T$	$\overline{Nu}_B$	$\overline{Nu}_L$	$\overline{Nu}_R$
		Case I	Case II	Case III	Case IV
10	[33]	1.158	4.860	8.638	8.118
	obtained	1.137281	4.835423	8.684453	8.058267
1.0	[33]	1.754	5.750	9.314	9.278
	obtained	1.717563	5.719602	9.371140	9.225091
0.1	[33]	10.393	12.161	13.047	11.343
	obtained	10.351011	12.124235	12.988560	11.295587

different solid volume fractions, φ, of nanofluid and its results compared with that of Ghasemi *et al*. [32] is shown in tab. 4. Further, in 3rd test case mixed convection flow in a lid-driven enclosure for four different cases (average Nusselt number at top wall –$\overline{Nu}_T$, average Nusselt number at bottom wall –$\overline{Nu}_B$, average Nusselt number at left wall –$\overline{Nu}_L$, average Nusselt number at right wall –$\overline{Nu}_R$) of isothermal heating or cooling is validated against the numerical results of Cheng and Liu [33], tab. 5. As shown in tabs. 3-5, there is a good agreement between the present results and their existing results in literature.

Results and discussion

The problem of MHD mixed convection in a Ag-water nanofluid (with $\varphi = 0.06$) filled square porous enclosure with a center heater at two positions is investigated for a range of heater length ($0.25 < \Gamma < 0.75$), Hartmann number ($0 < Ha < 50$), Richardson number ($0.01 < Ri < 100$), and Darcy number ($10^{-5} < Da < 10^{-1}$). The effect of all these active parameters are portrayed in streamlines, isotherms, velocity and average Nusselt number graphs. The following are the major significance of Ag-water nanofluid concerned in this present study. Adding Ag nanoparticles within the base fluid enhances the thermal conductivity of solid-fluid mixture when comparing with adding other nanofluids like Cu, CuO, TiO_2, and Al_2O_3. Heat transfer rate increases more with increase in the volume fraction of Ag-water nanofluid compared with other nanoparticles. The high level viscosity of the Ag-water nanofluid enhances diffusion of the momentum in nanofluid. The skin friction coefficient in the case of Ag-water nanofluid is bigger than that of a Cu-water nanofluid by increasing φ. At low porous layer thickness, Ag-water nanofluid appears with a higher enhancement in the heat transfer rate compared to other nanoparticles.

Figure 3 shows the effect of Darcy number and different length of horizontal heater at Ha = 25 and Ri = 1.0 on fluid-flow and temperature inside the enclosure. The Darcy number,

which is directly proportional to the permeability of the porous medium, is set to 10^{-5}, 10^{-3}, and 10^{1}. In general, for low Darcy number (Da = 10^{-5}) the flow circulation as well as thermal penetration are progressively inhibited due to reduced permeability of porous medium. The streamline contour for $\Gamma = 0.25$ and Da = 10^{-5} shows the primary circulation occupies most of the enclosure and strength of circulation is weak as the maximum streamline value is 0.002 at Da = 10^{-5}. It is interesting to notice that the flow characteristics coupled with temperature distribution at Ri = 1.0, Ha = 25 is limit. However, intensity of flow and temperature are not strongly coupled at smaller Darcy number. Even though by increasing heater length, penetration of heat is less due to less thermal diffusivity.

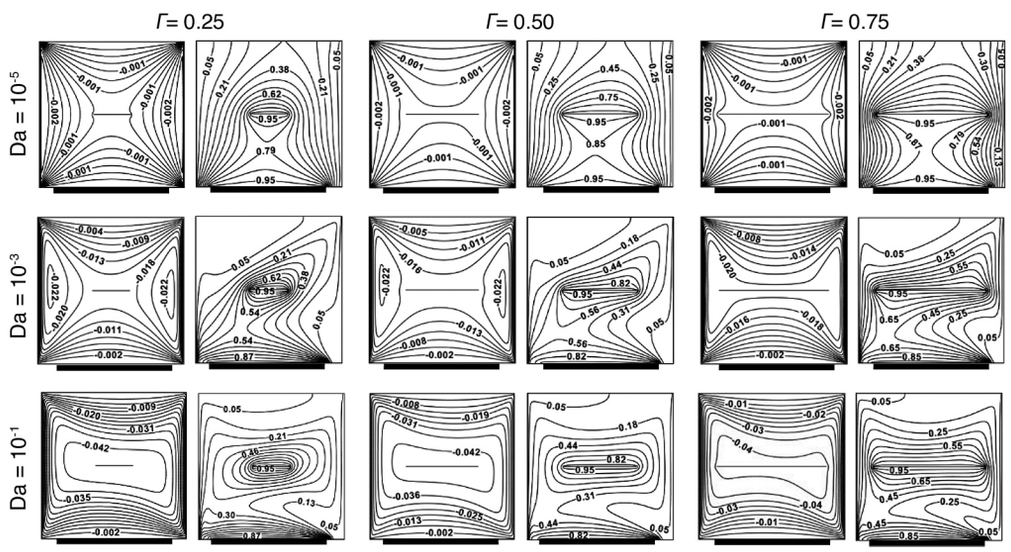

Figure 3. Streamlines and isotherms for different Darcy numbers and different length of horizontal heater at Ri = 1.0 and Ha = 25

Moreover, flow intensity is quite less at low Darcy number (Da = 10^{-5}) because a small size of porous layer has low permeability which permits very small amount of heat to transfer within the porous medium and hence the low Darcy number minimizes the average Nusselt number values. Therefore, the temperature distribution is similar to that with stationary fluid yield minimum heat transfer.

As Darcy number increases to Da = 10^{-3}, the strength of the flow is increased. As expected due to cold vertical moving walls, fluids rise up from middle portion of the bottom hot wall and flow down along the vicinity of two vertical walls forming symmetric rolls with clockwise and anticlockwise rotations near the moving vertical walls. The stronger circulation causes the temperature contours to be concentrated around the heater for its increasing length which may results in greater heat transfer due to the mixed convection. The streamlines for Da = 10^{-1} and $\Gamma = 0.25$ shows the enhancement of streamline intensities thereby assisting clockwise circulating flow which cause the streamline to be more active due to the vertical wall movement in the opposite directions. This results in expanding the flow at central region horizontally for which the convection significantly influences the overall heat transfer process. As the heater length increases the flow circulation becomes much stronger which corresponds to the occurrence of thermal stratification above and below the center heater produces more heat transfer.

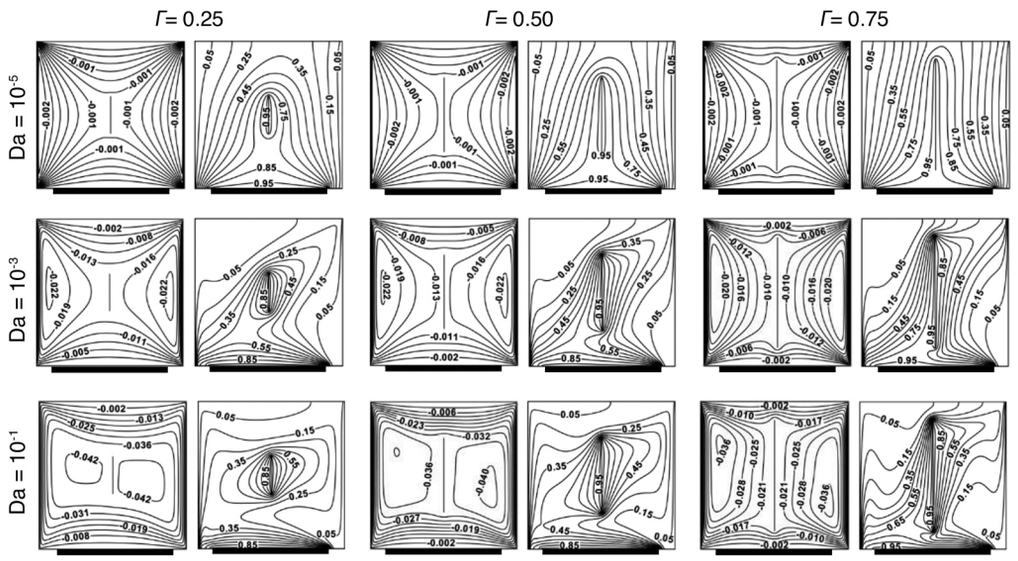

Figure 4. Streamlines and isotherms for different Darcy numbers and different length of vertical heater at Ri = 1.0 and Ha = 25

The effect of Darcy number on the flow patterns and isotherms inside the enclosure at Ha = 25, Ri = 1.0 for varying vertical heater length is elucidated in fig. 4. As Darcy number increases, the resistance to the flow caused by the presence of porous medium decreases. This causes the velocity of the fluid in the enclosure to increase. When Darcy number increases from 10^{-5} to 10^{-1} for heater length $\Gamma = 0.25$ the permeability of the porous medium increases causing the flow to ascend strongly. Also, it is interesting to notice the existence of the symmetric flow caused by the vertical walls moved in the opposite directions. Moreover, it is important to notice that increasing heater length strengthens the flow circulation for all increasing Darcy number values. Their corresponding isotherm plots shows that for low Darcy number value (Da = 10^{-5}), the convection heat transfer is minimum because of the retardation of the nanofluid flow. As a result, the isotherm contours are distributed throughout the enclosure with $\theta \leq 0.05$ near the vertical moving walls for all length of heaters.

As Darcy number increases to 10^{-3} the isotherm contours move towards the right top of enclosure as the shear force acting in the same direction with the buoyancy force at the right wall. For the further increase in Darcy number (Da = 10^{-1}) the isotherm lines around the heater becomes more dense with increased values of $\theta = 0.85$ and $\theta = 0.95$ which confirms the high heat transfer process is carried out by a mixed convection mechanism and high permeability of porous medium.

The mixed convective flow behavior is precised in fig. 5 in terms of mid height vertical velocity profile for horizontal heater of length $\Gamma = 0.75$. The presence of strong re-circulation flow for horizontal heater with length $\Gamma = 0.75$ at Ha = 0 is evident from this profile and also it is clear that the increasing Hartmann number results to slow down the fluid velocity.

Figure 6 illustrate the mid height vertical velocity profile for vertical heater with length $\Gamma = 0.75$, Ri = 1.0 and Da = 10^{-3}. This figure clearly shows that velocity magnitude decreases with increasing of Hartmann number. In general, magnetic field retards the flow velocity and trend of velocity profiles decreases with increasing Hartmann number.

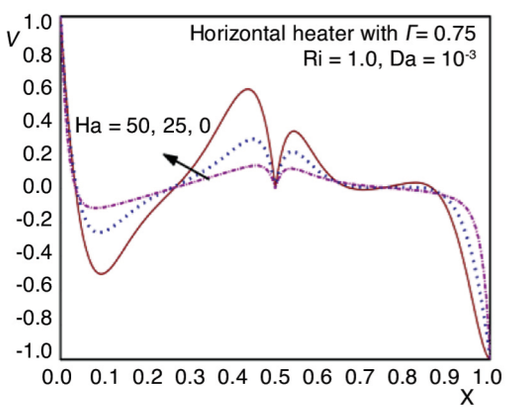

Figure 5. Mid height vertical velocity profile for different Hartmann numbers for horizontal heater with length $\Gamma = 0.75$, Ri = 1.0, and Da = 10^{-3}

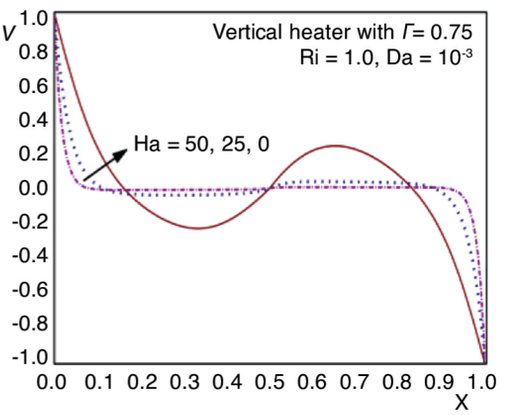

Figure 6. Mid height vertical velocity profile for different Hartmann numbers for vertical heater with length $\Gamma = 0.75$, Ri = 1.0, and Da = 10^{-3}

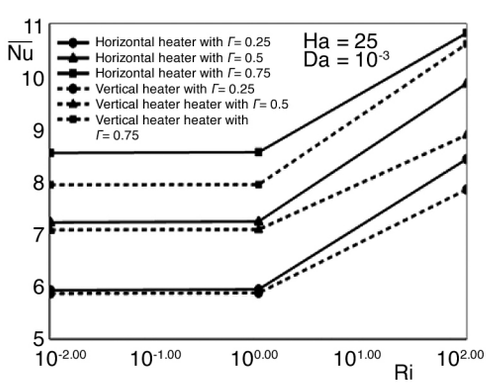

Figure 7. Variation of average Nusselt number *vs.* Richardson number for different length of both horizontal and vertical heater at Ha = 25 and Da = 10^{-3}

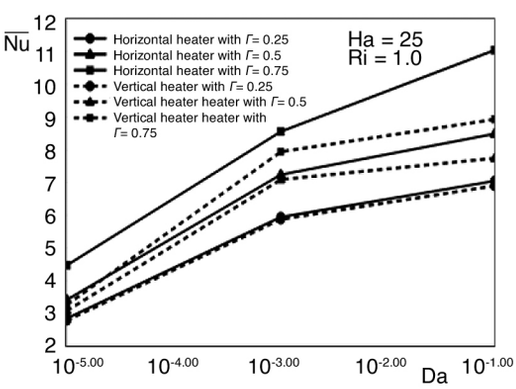

Figure 8. Variation of average Nusselt number *vs.* Darcy number for different length of both horizontal and vertical heater at Ha = 25 and Ri = 1.0

The average Nusselt number is plotted in fig. 7 for different Richardson number and different length of both horizontal and vertical heater. Generally average Nusselt number increases with increasing Richardson number as the length of the heater increases.

When Richardson number increases from 0.01 to 1.0 the average Nusselt number increases moderately for increasing heater length of both type. But for increments in Richardson number from 1.0 to 100 the average Nusselt number increases more because the transfer of heat in natural convection regime (Ri = 100) is more for the vertical wall movements compared with mixed convection regime. It is also found that maximum heat transfer rate is obtained for horizontal heater with length $\Gamma = 0.75$ when compared with vertical heater of maximum length. Figure 8 illustrates the variation of average Nusselt number with Darcy numbers for different length of both horizontal and vertical heater at Ha = 25 in the mixed convection regime. As seen from this figure average Nusselt number increases gradually along with the increasing Darcy number. In particular maximum heat transfer rate is attained for horizontal heater with length $\Gamma = 0.75$ at high Darcy number Da = 10^{-1} as large size of porous layer has high permeability which permits enormous amount of heat to transfer within the porous medium.

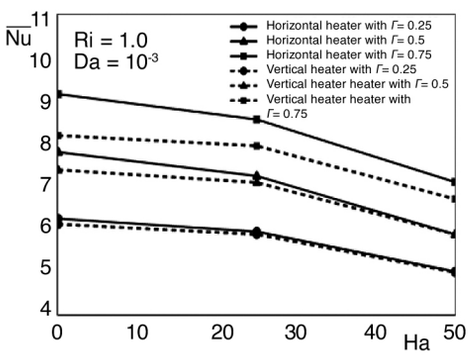

Figure 9. Variation of average Nusselt number *vs*. Hartmann number for different length of both horizontal and vertical heater at Ri = 1.0 and Da = 10^{-3}

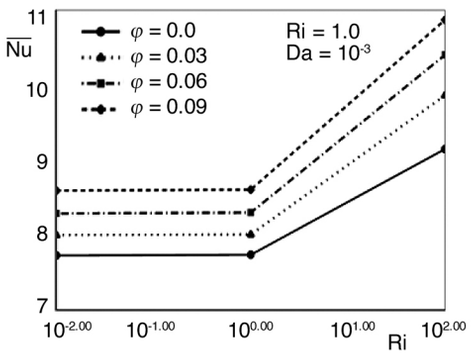

Figure 10. Variation of average Nusselt number *vs*. Richardson number for different solid volume fraction of nanoparticles at Ha = 25 and Da = 10^{-3}

In order to acquire the effect of varying heater length on MHD mixed convection, variation of average Nusselt number *vs*. Hartmann number is shown in fig. 9 for Ri = 1.0 and Da = 10^{-3}. The heat transfer rate increases for increasing heater length in the absence of magnetic field. We observe that the heat transfer rate decreases for increasing Hartmann number values due to the suppression of the convective recirculating flow within the enclosure. We also observe that there is no much difference in heat transfer rate for vertical and horizontal heater of length Γ = 0.25 and 0.5 in the presence of strong magnetic field whereas a considerable deviation in decreasing heat transfer rate is observed for maximum length of both type of heaters. The influence of solid volume fraction, ϕ, of nanoparticles on average Nusselt number *vs*. different Richardson numbers for horizontal heater (Γ = 0.75) is displayed in fig. 10 at Ha = 25 and Da = 10^{-3}. It is clearly observed that adding nanoparticles in the base fluid inside the porous enclosure cause an increase in the average Nusselt number. Also rate of increment on heat transfer clearly depends on the value of Richardson number. It is also evident from this figure that value of average Nusselt number grows as a percentage of nanoparticles increases from 0 to 9. This means that the addition of nanoparticles causes enhancement of the heat transfer for all considered values of Richardson number.

Conclusions

A computational study of MHD mixed convection in the porous enclosure filled with Ag-water nanofluid with center heater under the effect of magnetic field is conducted. The results are obtained for a wide range of pertinent dimensionless groups such as Darcy, Richardson, and Hartmann numbers. In view of the obtained results, the following findings are precised.

- The flow characteristics and heat transfer mechanism inside the enclosure are strongly dependent on the Richardson number.
- Significant changes occur in the flow and thermal fields for both vertical and horizontal heater at Ri = 100 which cause high heat transfer.
- As heater length increases average Nusselt number also increases. In particular, high heat transfer is attained for horizontal heater with length Γ = 0.75.
- Better heat transfer rate is achieved for Da = 10^{-1} which results the expected convective heat transfer inside the enclosure.
- The significant suppression of the convective current in the enclosure is due to increase of Hartmann number.

- The velocity of the fluid flow augmented by the increase of solid volume fraction of nanoparticle which results increase in heat transfer rate.

Nomenclature

B_0 – strength of magnetic field
c_p – specific heat, [$Jkg^{-1}K^{-1}$]
Da – darcy number
g – gravitational acceleration, [ms^{-2}]
Gr – grashot number
Ha – hartmann number
h – heat transfer coefficient, [$Wm^{-2}K$]
K – permeability of porous medium
k – thermal conductivity, [$Wm^{-1}K^{-1}$]
L – enclosure height and width [m]
l – dimensional length of heat source
Nu – local Nusselt number
$\overline{Nu}$ – average Nusselt number
P – dimensionless pressure
p – dimensional pressure, [Nm^{-2}]
Pr – prandtl number
q'' – heat flux at the source
Re – reynolds number
Ri – richardson number
T – dimensional temperature, [K]
U,V – dimensionless velocity components
u,v – dimensional velocity components, [ms^{-1}]
X,Y – dimensionless cartesian coordinates
x,y – dimensional cartesian coordinates, [m]

Greek symbol

α – thermal diffusivity, [m^2s^{-1}]
β – thermal expansion coefficient, [$K^{-2}L$]
Γ – dimensionless length of the heater
γ – dimensional length of the heater, [m]
ε – dimensionless length of heat source, [l/L]
θ – dimensionless temperature
μ – dynamic viscosity, [$Kgm^{-1}s^{-1}$]
υ – kinematic viscosity, [m^2s^1]
ρ – density, [Kgm^{-3}]
σ – electrical conductivity, [Sm^{-1}]
φ – volume fraction of the nanoparticles

Subscript

c – cold wall
f – fluid
h – hot wall
nf – nanofluid
s – solid nanoparticles

References

[1] Bejan, A., *et al., Porous and Complex Flow Structures in Modern Technologies*, Springer, New York, USA, 2004
[2] Vafai, K., *Handbook of Porous Media*, 2rd ed., Taylor and Francis, New York, USA, 2005
[3] Ingham, D. B., Pop I., *Transport Phenomena in Porous Media*, Elsevier, Oxford, UK, 2005
[4] Nield, D., Bejan, A., *Convection in Porous Media*, Springer, 3rd ed., Berlin, Germany, 2006
[5] Khanafer, K., Vafai, K., Double-Diffusive Mixed Convection in a Lid-Driven Enclosure Filled with a Fluid-Saturated Porous Medium, *Numerical Heat Transfer*, Part A, *42* (2002), 5, pp. 465-486
[6] Mahmud, S., Pop, I., Mixed Convection in a Square Vented Enclosure Filled with a Porous Medium, *Int. J. Heat Mass Transfer*, *49* (2006), 13-14, pp. 2190-2206
[7] Jaballah, S., *et al.,* Numerical Simulation of Mixed Convection in a Channel Irregularly Heated and Partially Filled with a Porous Medium, *J. Por. Media*, *11* (2008), 3, pp. 247-257
[8] Basak, T., *et al*., A Peclet Number Based Analysis of Mixed Convection for Lid-Driven Porous Square Cavities with Various Heating of Bottom Wall, *Int. Comm. Heat Mass Transfer*, *39* (2012), 5, pp. 657-664
[9] Rahman, M.M., *et al*., Unsteady Mixed Convection in a Porous Media Filled Lid-Driven Cavity Heated by a Semi-Circular Heaters, *Thermal Science*, *19* (2015), 5, pp. 1761-1768
[10] Mittal, N., *et al*., Numerical Simulation of Mixed Convection in a Porous Medium Filled with Water / Al_2O_3 Nanofluid, *Heat Transfer - Asian Research*, *42* (2013), 1, pp. 46-59
[11] Heydari, M. R., *et al*., Mixed Convection Heat Transfer in a Double Lid-Driven Inclined Square Enclosure Subjected to Cu-Water Nanofluid with Particle Diameter of 90 nm, *Heat Transfer Research, 45* (2014), 1, pp. 75-95
[12] Kefayati, G. H. R., FDLBM Simulation of Magnetic Field Effect on Mixed Convection in a Two Sided Lid-Driven Cavity Filled with Non-Newtonian Nanofluid, *Powder Technol*., *280* (2015), Avg. pp. 135-153
[13] Nayak, R. K., *et al*., Numerical Study on Mixed Convection and Entropy Generation of a Nanofluid in a Lid-Driven Square Enclosure, *J. Heat Transfer, 138* (2016), 1, pp. 012503-1 - 012503-11
[14] Sheikholeslami, M., Influence of Lorentz Forces on Nanofluid Flow in a Porous Cavity by Means of Non-Darcy Model, *Engineering Computations, 34* (2017), 8, pp. 2651-2667
[15] Sheikholeslami, M., Rokni, H. B., Simulation of Nanofluid Heat Transfer in Presence of Magnetic Feld: A Review, *International Journal of Heat and Mass Transfer*, *115* (2017), Part B, pp. 1203-1233

[16] Sheikholeslami, M., Bhatti, M.M., Forced Convection of Nanofluid in Presence of Constant Magnetic Field Considering Shape Effects of Nanoparticles, *International Journal of Heat and Mass Transfer*, *111* (2017) Aug., pp.1039-1049
[17] Oztop, H. F., *et al*., Comparision of Position of a Heated Thin Plate Located in a Cavity for Natural Convection, *Int. Comm. Heat Mass Transfer*, *31* (2004), 1, pp. 121-132
[18] Dogan, M., Sivrioglu, M., Experimental Investigation of Mixed Convection Heat Transfer from Longitudinal Fins in a Horizontal Rectangular Channel: In Natural Convection Dominated Flow Regimes, *Energy Conversion and Management*, *50* (2009), 10, pp. 2513-2521
[19] Islam, A. W., *et al*., Mixed Convection in a Lid Driven Square Cavity with an Isothermally Heated Square Blockage Inside, *Int. J. Heat Mass Transfer*, *55* (2012), 19-20, pp. 5244-5255
[20] Kalteh, M., *et al*., Numerical Solution of Nanofluid Mixed Convection Heat Transfer in a Lid-Driven Square Cavity with Triangular Heat Source, *Powder Technol*. *253* (2014), Feb., pp. 780-788
[21] Rahman, M. M., *et al*., MHD Mixed Convection with Joule Heating Effect in a Lid-Driven Cavity with a Heated Semi-Circular Source Using the Finite Element Technique, *Numerical Heat Transfer*, *60* (2011), 6, pp. 543-560
[22] Selimefendigil, F., Oztop, H. F., Numerical Study of MHD Mixed Convection in a Nanofluid Filled Lid Driven Square Enclosure with a Rotating Cylinder, *Int. J. Heat Mass Transfer*, *78* (2014), Nov., pp. 741-754
[23] Abu-Nada, E., Dissipative Particle Dynamics Simulation of Combined Convection in a Vertical Lid Driven Cavity with a Comer Heater, *Int. J. Therm. Sci., 92* (2015), C., pp. 72-84
[24] Rahman, M. M., *et al.,* Unsteady Mixed Convection in a Porous Media Filled Lid-Driven Cavity Heated by a Semi-Circular Heaters, *Thermal Science, 19* (2015), 5, pp. 1761-1768
[25] Gangawane, K. M., Computational Analysis of Mixed Convection Heat Transfer Characteristics in Lid-Driven Cavity Containing Triangular Block with Constant Heat Flux: Effect of Prandtl and Grashof numbers, *Int. J. Heat Mass Transfer*, *105* (2017), Feb., pp. 34-57
[26] Sheikholeslami, M., Sadoughi, M. K., Simulation of CuO-Water Nanofluid Heat Transfer Enhancement in Presence of Melting Surface, *Int. Comm. Heat Mass Transfer*, *116* (2018), Jan., pp. 909-919
[27] Mahmoodi, M., Numerical Simulation of Free Convection of Nanofluid in a Square Cavity with an Inside Heater, *Int. J. Therm. Sci., 50* (2011), 11, pp. 2161-2175
[28] Patankar, S.V., *Numerical Heat Transfer and Fluid Flow*, Hemisphere Publishing Corporation, New York, USA, 2004
[29] Nithyadevi, N., Rajarathinam, M., Effect of Inclination Angle and Magnetic Field on Convection Heat Transfer for Nanofluid in a Porous Cavity, *Journal of Applied Fluid Mechanics, 9* (2016), 5, pp. 2347-2358
[30] Umadevi, P., Nithyadevi, N., Magneto-Convection of Water-Based Nanofluids Inside an Enclosure Having Uniform Heat Generation and Various Thermal Boundaries, *Journal of the Nigerian Mathematical Society, 35* (2016), 1, pp. 82-92
[31] Nithyadevi, N., *et al.*, Effects of Inclination Angle and Non-Uniform Heating on Mixed Convection of a Nanofluid Filled Porous Enclosure with Active Mid-Horizontal Moving, *International Journal of Heat and Mass Transfer, 104* (2017), Jan., pp.1217-1228
[32] Ghasemi, B., *et al*., Magnetic Field Effect on Natural Convection in a Nanofluid-Filled Square Enclosure, *Int. J. Therm. Sci*., *50* (2011), 9, pp. 1748-1756
[33] Cheng, T. S., Liu, W. H., Effect of Temperature Gradient Orientation on the Characteristics of Mixed Convection Flow in a Lid-Driven Square Cavity, *Comput. Fluids*, *39* (2010), 6, pp. 965-978

Paper submitted: November 5, 2017
Paper revised: December 5, 2017
Paper accepted: December 6, 2017

© 2019 Society of Thermal Engineers of Serbia.
Published by the Vinča Institute of Nuclear Sciences, Belgrade, Serbia.
This is an open access article distributed under the CC BY-NC-ND 4.0 terms and conditions.